

# FLARELIKE BRIGHTENINGS OF ACTIVE REGION LOOPS OBSERVED WITH SUMER

T. J. Wang, D. E. Innes, S. K. Solanki, and W. Curdt

Max-Planck-Institut für Sonnensystemforschung, 37191 Katlenburg-Lindau, Germany  
email: wangtj@mps.mpg.de

1

## ABSTRACT

Coronal loops on the east limb of the Sun were observed by SUMER on SOHO for several days. Small flare-like brightenings are detected very frequently in the hot flare line Fe XIX. We find that the relatively intense events are in good coincidence with the transient brightenings seen by Yohkoh/SXT. A statistical analysis shows that these brightenings have durations of 5-84 min and extensions along the slit of 2-67 Mm. The integrated energy observed in Fe XIX for each event is in the range of  $3 \times 10^{18} - 5 \times 10^{23}$  ergs, and the estimated thermal energy ranges from  $10^{26} - 10^{29}$  ergs. Application of the statistical method proposed by Parnell & Jupp (2000) yields a value of 1.5 to 1.8 for the index of a power law relation between the frequency of the events and the radiated energy in Fe XIX, and a value of 1.7 to 1.8 for the index of the frequency distribution of the thermal energy in the energy range  $> 10^{27}$  ergs. We examine the possibility that these small brightenings give a big contribution to heating of the active region corona.

Key words: solar flares; coronal heating; UV radiation, X-rays.

## 1. INTRODUCTION

It is well known that there is not enough energy in large flares to heat the corona because they are so rare that their time-averaged power contribution is too small. However, a multitude of small-scale reconnection events (microflares or nanoflares) may be a possible source for heating the corona (e.g., Levine 1974; Parker 1988). Balloon-borne observations of many small

hard X-ray bursts with energies between  $10^{24} - 10^{27}$  ergs by Lin et al. (1984) seem to support this idea. Systematic detection and statistical analysis of small-scale phenomena in the corona have been explored in recent years with soft X-ray and EUV high-resolution imaging telescopes such as Yohkoh/SXT, SOHO/EIT and TRACE (see a review by Aschwanden 2004). Active region transient brightenings (ARTBs) (e.g. Shimizu et al. 1992) and X-ray bright points (XBP) in the quiet Sun (e.g. Golub et al. 1974) are governed by flare-like processes and release thermal energy comparable to hard X-ray microflares. EUV transient brightenings in the quiet Sun with temperatures of 1-2 MK and energies of  $10^{24} - 10^{27}$  ergs were first studied with SOHO/EIT data (e.g. Krucker & Benz 1998) and with TRACE data (e.g. Parnell & Jupp 2000). It appears that these transient EUV brightenings have all the properties of larger flares, indicative of a continuous distribution of energy release in the corona from large flares down to tiny nanoflares.

The frequency distribution of the energy release can be used to examine the microflare or nanoflare heating hypothesis. Hudson (1991) showed that in order to explain the heating of the corona by microflares or nanoflares, the frequency distribution of small energy release events must be a power law with index steeper than 2. In many of the early papers (see a review by Crosby et al. 1993), the index of the frequency of regular flares was estimated to be around 1.8 by assuming that the energy in a flare is linearly related to the peak flux of the flare. Crosby et al. (1993) calculated the distribution of the total nonthermal energy using hard X-ray bremsstrahlung observations, and found a value of 1.53 for the index of event energies in the range  $10^{28} - 10^{31}$  ergs. Shimizu (1995) studied ARTBs with energies in the range  $10^{27} - 10^{29}$  ergs, and they estimated the index for the energy distribution to be 1.5-1.6. For the EUV nanoflares detected by SOHO/EIT and TRACE, many estimates were made for the index with results between 1.4 and 2.6 (see reviews by Aschwanden 2004; Parnell 2004). This clearly shows nanoflare heating of the corona remains an open question.

In this paper, we study hot flare-like brightenings which frequently occur in coronal loops as seen in SUMER

<sup>1</sup>Proceedings of the 11th European Solar Physics Meeting "The Dynamic Sun: Challenges for Theory and Observations" (ESA SP-600). 11-16 September 2005, Leuven, Belgium. Editors: D. Danesy, S. Poedts, A. De Groof and J. Andries. Published on CDROM., id.105.1

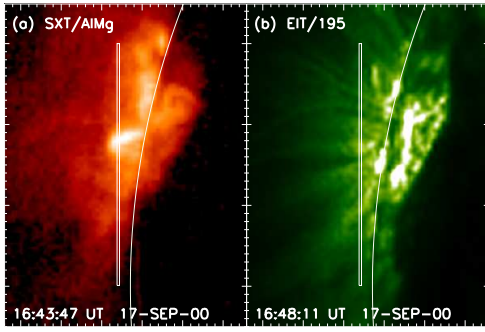


Figure 1. **a)** Image of loop systems in AR 9167 and AR 9169 observed with SXT AlMgMn-sandwich filter. The offlimb position of the SUMER slit is marked as a narrow box. **b)** The same region observed with EIT 195Å filter.

spectra taken 10 to 40 Mm above active regions on the limb. We first make a multi-wavelength analysis of these events, then we make a statistical study of their physical properties and calculate frequency distributions of their peak intensities and energies to explore whether the contribution of these events is important in heating the active-region corona.

## 2. OBSERVATIONS

The data sets analyzed include two observations which were made by the SUMER spectrometer in the sit-and-stare mode (see Fig. 1). The first observation was recorded with a cadence of 90 s and the  $300'' \times 4''$  slit during 16–20 September 2000. Five spectral lines were transmitted, including Fe XIX  $\lambda$  1118 (6.3 MK), Ca XV  $\lambda$  1098 and  $\lambda$  555 $\times$ 2 (3.5 MK), Ca XIII  $\lambda$  1134 (2.2 MK), and Si III  $\lambda$  1113 (0.06 MK). The second observation was made with a cadence of 162.5 s during 25–30 September 2000. A transmitted spectral window covering 1097–1119 Å contains a number of lines formed in the temperature range 0.01–10 MK, e.g. Fe XIX  $\lambda$  1118, Ca XV  $\lambda$  1098, Al XI  $\lambda$  550 $\times$ 2 (1.6 MK), Ca X  $\lambda$  557 $\times$ 2 (0.7 MK), Ne VI  $\lambda$  558 $\times$ 2 (0.3 MK), and Si III  $\lambda$  1113.

## 3. RESULTS: MULTIWAVELENGTH ANALYSIS

We first compare Fe XIX Brightenings with GOES Flares. Figure 2 shows such an example. We find that 40 of 53 Fe XIX enhancements, which are identified from light curves on 16–19 Sep and 25–28 Sep 2000, coincide in time with GOES C-class flares. Note that many of these brightenings are associated with longitudinal loop oscillations seen in the Fe XIX line (Innes & Wang 2004). We find that all major brightenings seen in Fe XIX are also clearly seen in SXT emission, indicating that the emission seen by SUMER in the Fe XIX line and the SXT brightenings are signatures of the same phenomena. Fig-

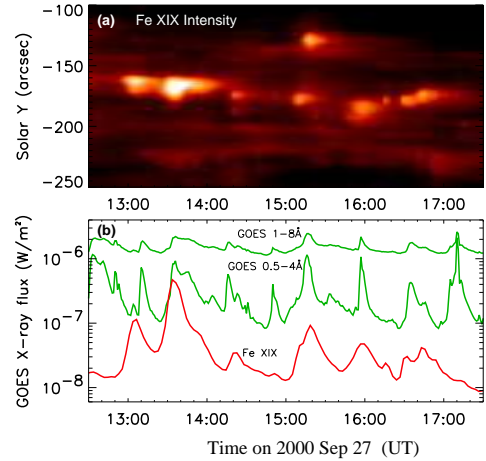


Figure 2. **a)** Intensity time series of the Fe XIX line detected at the upper part of the slit. **b)** Light curve of the Fe XIX line integrated along the slit in arbitrary units. Light curves of GOES full-sun soft X-ray flux through 1–8 Å and 0.5–4 Å are also plotted. The flux of GOES 0.5–4 Å is multiplied by a factor of 10.

ure 3 shows such an example. However, a long succession of SUMER observations is preferable to do a complete statistical study, over SXT data with gaps.

Figure 4 illustrates the cooling of Fe XIX brightenings into the 195 Å EIT filter (1.5 MK). For 12 strong Fe XIX brightenings, Their average cooling times from Fe XIX to Ca XV, Ca XIII (or Al XI), and EIT 195Å filter temperatures are 27 min, 53 min, and 70 min for limb loops at a projected height of  $\sim 30$  Mm. We find that most of the Fe XIX brightenings have no counterparts seen in the low ( $< 4$  MK) temperature lines. There are two explanations. One is due to the obscuration by strong background emission in the normal coronal lines. The other is because coronal loops in the AR core are generally at 5–8 MK (Yoshida & Tsuneta 1996), so do not cool to lower temperatures.

## 4. RESULTS: STATISTICAL ANALYSIS

### 4.1. Identification of Brightening Events by Automatic Search

We first remove the background emission and determine the noise level ( $\sigma$ ) at each pixel position. In order to make an automatic search, we define the following criterion for an event:

- 1)  $I_{dif} > N\sigma$ , where  $I_{dif}$  is the enhancement of peak intensity relative to the minimum intensities preceding and following the event. This condition defines an event for a single pixel.
- 2)  $\Delta T_p \leq N\Delta t$ , where  $\Delta T_p$  is the time difference between peak intensities at two neighboring pixels,  $\Delta t$  is the time cadence. This step groups together the neighboring spatial pixels which peak almost simultaneously.

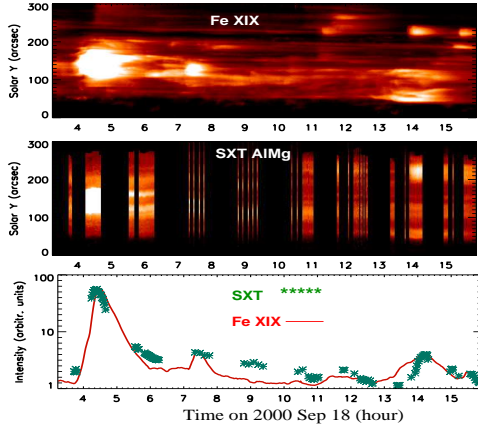


Figure 3. **a)** Intensity time series of the Fe XIX line detected at the slit. **b)** Same as **a)** but for the SXT AlMgMn-sandwich filter. **c)** Light curves of the Fe XIX line and the SXT AlMgMn filter integrated over the slit.

3)  $L_y \geq N$  pixels, where  $L_y$  is the extension of events along the slit. In this step, we separate the neighboring events along the slit according to their peak intensity variation, and define the smallest events which should fulfil the given condition.

#### 4.2. Physical Condition of Brightenings

We have identified in total 1334 events matching the criteria  $I_{dif} > 1\sigma$ ,  $\Delta T_p \leq 3\Delta t$ , and  $L_y \geq 3$  pixels from the two data sets with a total observing duration of 96.6 hours. Figure 5 shows such an example. We calculate the duration of an event at a single pixel as the FWHM of an enhancement in intensity relative to its preceding minimum. We define the duration of each event as the average value of durations for all spatial pixels in this event and define the extension of each event along the slit as the scale of all grouped pixels making this event. We obtain a mean duration of  $22 \pm 13$  min ranging from 5-84 min, and a mean extension  $L_y$  of  $7 \pm 6$  Mm ranging from 2-67 Mm. The peak intensity of events has a mean of  $0.03 \pm 0.12$  W/m<sup>2</sup> in the range  $10^{-4}$ -2.2 W/m<sup>2</sup>. Under the assumption that the temperature at peak intensity is at a value of 6.3 MK, i.e. the temperature where the emissivity reaches the maximum ( $G_{max}$ ), we can estimate the emission measure by  $I_{peak}/G_{max}$ . We calculated that the emission measure of brightenings has a mean of  $(0.3 \pm 1.4) \times 10^{28}$  cm<sup>-5</sup> in the range  $10^{25}$ - $2.5 \times 10^{29}$  cm<sup>-5</sup>. Assuming a constant line-of-sight depth of 10 Mm, we estimated that the electron density has a mean of  $(1.1 \pm 1.3) \times 10^9$  cm<sup>-3</sup> in the range  $10^8$ - $1.6 \times 10^{10}$  cm<sup>-3</sup>. To estimate the thermal energy content for each event, we need to know the loop geometry. Assuming that the temperature of brightening loops is 6 MK, the loop length ( $L$ ) is 3 times  $L_y$  and the loop width ( $w$ ) is 10 Mm, we estimate the thermal energy by  $E_{th} = 3n_e k_B T (Lw^2)$ . We obtained that  $E_{th}$  has a mean of  $(7.9 \pm 19) \times 10^{27}$  ergs in the range  $1.8 \times 10^{26}$ - $2.5 \times 10^{29}$  ergs. The integrated

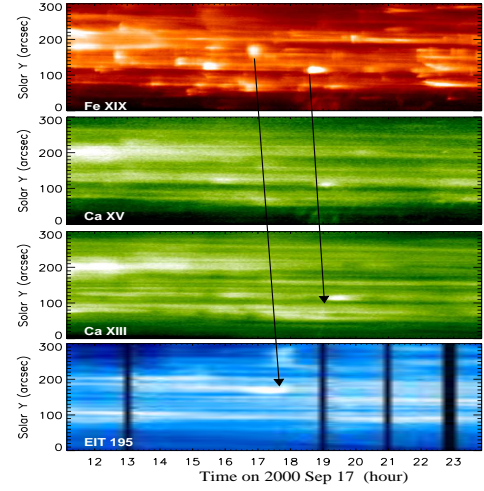


Figure 4. Line-integrated intensity time series of **a)** the Fe XIX line, **b)** the Ca XV line, **c)** the Ca XIII line, and **d)** the EIT 195 Å filter, detected at the slit. The arrows demonstrate the cooling of two hot brightenings seen in Fe XIX and with a time delay as low-temperatures brightenings.

energy of brightenings observed in the Fe XIX line has a mean of  $(5.4 \pm 27) \times 10^{21}$  ergs in the range  $2.8 \times 10^{18}$ - $5.1 \times 10^{23}$  ergs.

#### 4.3. Frequency Distributions

Assuming that the distribution of the peak intensities or energies follows a power-law, i.e.,

$$f(E) = \frac{f_0}{E_0} \left( \frac{E}{E_0} \right)^{-\alpha}, \quad (1)$$

we determine the index,  $\alpha$ , by using the maximum likelihood method proposed by Parnell & Jupp (2000). We obtained  $\alpha \approx 1.7$  for the peak intensity distribution and  $\alpha=1.5$ -1.8 for the frequency distribution of the radiated energy observed in Fe XIX. For the thermal energies estimated based on the assumption of  $L/L_y = 3$ , we obtained  $\alpha=1.7$ -1.8 in the energy range greater than  $10^{27}$  ergs. We also made a test to calculate the thermal energy of events by assuming  $L/L_y = f_i$ , where  $f_i$  ( $i=1,2, \dots, N$ ) are taken from a uniformly-distributed random series in the range 2-7. For 5 random series, we found the values of  $\alpha$  in the same range as the case of  $L/L_y = 3$ .

We can estimate the total energy rate by,

$$P = \int_{E_{min}}^{E_{max}} f(E) E dE. \quad (2)$$

If the distribution  $f(E)$  is a power-law (see Eq.(1)), then we have

$$P = \frac{f_0 E_0}{2 - \alpha} \left( \left( \frac{E_{max}}{E_0} \right)^{2-\alpha} - \left( \frac{E_{min}}{E_0} \right)^{2-\alpha} \right). \quad (3)$$

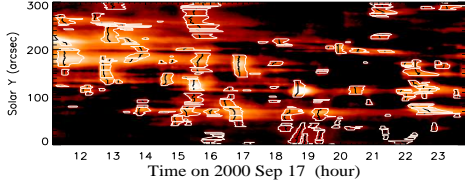


Figure 5. Example of the Fe XIX brightening identification with automatic search. The black curves mark the peak times of intensity in an event. The time series of the Fe XIX intensity shown here is the same as that in Fig. 4, but with the background removed.

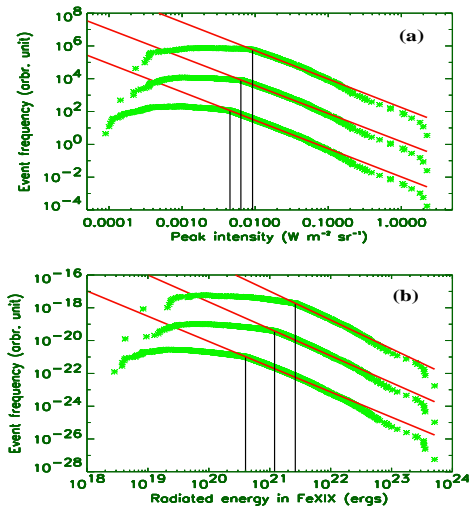


Figure 6. Frequency of events vs. **a)** event peak intensity, and **b)** event integrated energy in the Fe XIX line for events of intensity enhancements at least  $1\sigma$ ,  $2\sigma$ , and  $3\sigma$ . These plots show the observed data (in green color) and the right-hand power law of the fitted skew-Laplace distribution (red line). The frequencies of events for the three cases in **a)** and **b)** are multiplied by 1,  $10^2$ ,  $10^4$ , respectively, so they can all be drawn without overlap on the same graph.

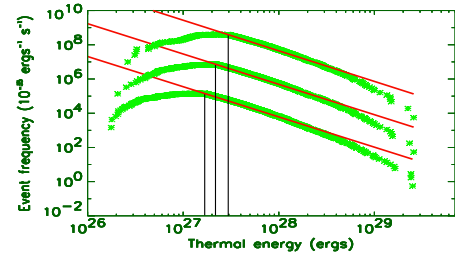


Figure 7. Frequency of events vs. event thermal energy. The thermal energy of an event is calculated by assuming the loop length to be three times the brightening extension along the slit. The frequencies of events for the three cases (with intensity enhancements at least  $1\sigma$ ,  $2\sigma$ , and  $3\sigma$ ) are multiplied by 1,  $10^2$ ,  $10^4$ , respectively.

Taking  $\alpha = 1.77$  for the case of  $I_{dif} > 1\sigma$  and  $1.8 \times 10^{26} < E_{th} < 2.5 \times 10^{29}$  ergs for the observed events, we obtained  $P = 5.6 \times 10^{25}$  ergs  $s^{-1}$ . If assuming that the power-law continues from  $10^{24}$  to  $10^{33}$  ergs, the upper limit of total energy supplied by these brightenings and flares was estimated to be about  $5 \times 10^{26}$  ergs  $s^{-1}$ , or  $5 \times 10^6$  ergs  $cm^{-2} s^{-1}$  for ARs of the size of 100 Mm. This energy input rate is close to but insufficient for the heating of the active-region corona, which has a typical energy loss rate of  $10^7$  ergs  $cm^{-2} s^{-1}$  (Withbroe & Noyes 1977).

## 5. CONCLUSION

There are many heating events in active region loops that can only be seen at temperatures greater than 6 MK, e.g. microflares recently detected by RHESSI revealing temperatures of 6-14 MK from the spectral fits in the 3-15 KeV energy range (Benz & Grigis 2002). We see them clearly in SUMER Fe XIX line emission. We estimate a power-law index of 1.7-1.8 for the frequency distribution of the thermal energies of these events in the range  $10^{27}$ - $10^{29}$  ergs. Their energy input rate does not seem to be sufficient for heating the active-region corona.

## REFERENCES

- Aschwanden, M. J. 2004, *Physics of the Solar Corona - An Introduction*, Chichester UK: Praxis Publishing Ltd, International Publishers in Science and Technology, and Berlin: Springer
- Benz, A. O., & Grigis, P. C. 2002, *Solar Phys.*, 210, 431
- Crosby, N. B., Aschwanden, M. J., & Dennis, B. R. 1993, *Solar Phys.*, 143, 275
- Golub, L., Krieger, A. S., Silk, J. K., Timothy, A. F., & Vaiana, G. S 1974, *ApJ*, 189, L93
- Hudson, H. S. 1991, *Solar Phys.*, 133, 357

- Innes, D. E., & Wang, T. J. 2004, *In Proc. 15th SOHO Workshop: Coronal Heating* eds. R. W. Walsh et al. (ESA SP-575, Noordwijk: ESA), p.553
- Krucker, S., & Benz, A. O. 1998, *ApJ*, 501, L213
- Levine, R. H. 1974, *ApJ*, 190, 457
- Lin, R. P., Schwartz, R. A., Kane, S. R., Pelling, R. M., & Hurley, K. C. 1984, *ApJ*, 283, 421
- Parker, E. N. 1988, *ApJ*, 330, 474
- Parnell, C. E., & Jupp, P. E. 2000, *ApJ* 529, 554
- Parnell, C. E. 2004, *In Proc. 15th SOHO Workshop: Coronal Heating*, eds. R. W. Walsh et al. (ESA SP-575, Noordwijk: ESA), p.227
- Shimizu, T., Tsuneta, S., Acton, L. W., Lemen, J. R., & Uchida, Y. 1992, *PASJ*, 44, L147
- Shimizu, T. 1995, *PASJ*, 47, 251
- Withbroe, G. L., & Noyes, R. W. 1977, *ARA&A*, 15, 363
- Yoshida, T., & Tsuneta, S. 1996, *ApJ*, 459, 342